Journal of General Virology (2002), **83**, 179–188. Printed in Great Britain

Latent nuclear antigen of Kaposi's sarcoma herpesvirus/human herpesvirus-8 induces and relocates RING3 to nuclear heterochromatin regions

Karin Mattsson,[1] Csaba Kiss,[1] Georgina M. Platt,[3] Guy R. Simpson,[3] Elena Kashuba,[1] George Klein,[1] Thomas F. Schulz[2,3] and Laszlo Szekely[1]

[1] Microbiology and Tumor Biology Center, Karolinska Institute, PO Box 280, S-171 77, Stockholm, Sweden

[2] Department of Virology, Hannover Medical School, D-30623 Hannover, Germany

[3] Molecular Virology Group, Department of Medical Microbiology, The University of Liverpool, UK

LANA, the major latency-associated nuclear antigen of Kaposi's sarcoma herpesvirus/human herpesvirus-8 (KSHV/HHV-8), binds RING3 protein, one of five human homologues of the *fsh* (female sterile homeotic) gene product of *Drosophila*. In KSHV/HHV-8-infected cells LANA and the viral episomes accumulate in heterochromatin-associated nuclear bodies. Here we show that in several KSHV/HHV-8-negative cell lines derived from carcinomas, sarcomas and lymphomas, RING3 was expressed at low levels, primarily localized to the euchromatin, and dissociated from the chromosomes during mitosis. In contrast, in KSHV/HHV-8-infected body cavity lymphoma cells the bulk of RING3 localizes to the LANA nuclear bodies and remains associated with the chromosomes during cell division. KSHV/HHV-8-infected body cavity lymphoma cells expressed RING3 at much higher levels than cells without the virus. Transfection of full-length LANA, but not the C terminus alone, greatly induced RING3 gene expression, and LANA and RING3 co-localized even in the transfected cells, in the absence of KSHV/HHV-8 viral DNA. High levels of LANA expression led to the disappearance of heterochromatin in both human and mouse cells. We suggest that LANA and RING3 may create a local euchromatic microenvironment around the viral episomes that are anchored to the heterochromatin.

Introduction

LANA is the major latency-associated nuclear antigen encoded by human herpesvirus-8 (Kedes *et al.*, 1997; Kellam *et al.*, 1997; Rainbow *et al.*, 1997). It is expressed at high levels in Kaposi's sarcoma herpesvirus/human herpesvirus-8 (KSHV/HHV-8)-infected Kaposi's sarcoma, body cavity lymphoma (BC; also called primary effusion lymphoma) cells, and cells of lymphadenopathy associated with multicentric Castleman's disease (Boshoff & Weiss, 1998; Rainbow *et al.*, 1997; Dupin *et al.*, 1999; Katano *et al.*, 1999). It accumulates in distinct nuclear bodies in KSHV/HHV-8-infected cells. Previously we have shown that the nuclear bodies are associated with the borders of heterochromatin in KSHV/HHV-8-positive BC cell lines, human–mouse hybrid cells and derivatives of the hybrids that had lost most of the human genetic material (Szekely *et al.*, 1999). LANA-containing nuclear bodies remain associated with the chromosomes during mitosis (Szekely *et al.*, 1998). LANA binds and anchors the circular viral DNA to the host cell chromatin during both the interphase and mitosis. LANA binds to the latent origin of replication of HHV-8 (Ballestas *et al.*, 1999). It is also able to bind histone H1, a possible target for the tethering of viral episomes to the mitotic chromosomes (Cotter & Robertson, 1999). In this respect it is reminiscent of the Epstein–Barr virus (EBV)-encoded latent nuclear antigen 1 (EBNA-1). However, LANA and EBNA-1 accumulate into distinct, non-overlapping, nuclear bodies in EBV/HHV-8 dually infected BC cells (Szekely *et al.*, 1998).

LANA is a nuclear phosphoprotein encoded by orf73 as part of a polycistronic message (Rainbow *et al.*, 1997). It is expressed in all latently infected cells and is considered to be one of the major viral proteins that contributes to cell transformation. It binds and inhibits the transcriptional trans-

Author for correspondence: Laszlo Szekely.
Fax +46 8 330498. e-mail lassze@ki.se

Table 1. Cellular distribution and staining intensity of RING3 in different cell lines

Cell line	RING3 staining pattern	
	Weak (homogeneous or fine speckled)	Intense (distinct nuclear bodies)
BCBL1 (HHV-8, EBV)		●
BC1 (HHV-8)		●
MCF7	●	
HeLa	●	
ECV	●	
SW480	●	
LCL 94C1	●	
LCL Nadia	●	
Akata (EBV$^-$)	●	
Akata (EBV$^+$)	●	
Mutu I	●	
Mutu III	●	
Rael	●	
Raji	●	
DG75	●	
Jurkat	●	
NKL92	●	
L cells (mouse)	●	

activating function of p53 and through this may protect cells from p53-induced apoptosis (Friborg *et al.*, 1999). LANA also binds the retinoblastoma (Rb) protein and activates E2F-dependent transcription. LANA alleviates the growth inhibitory effect of Rb on Saos cells and, together with HRas, transforms primary rodent fibroblasts (Radkov *et al.*, 2000). LANA associates with co-repressor protein SAP30, part of the mSin3 co-repressor complex that directs histone deacetylases to specific DNA sites (Krithivas *et al.*, 2000).

LANA can modulate the expression levels of several different synthetic or natural promoters of both viral and cellular origin. LANA up-regulates its own expression along with v-cyclin and v-FLIP and a set of interferon-responsive cellular genes. On the other hand it down-regulates expression from the human immunodeficiency virus long terminal repeat and also NF-κB-dependent reporter genes (Renne *et al.*, 2001). It also binds to RING3, one of five human homologues of *fsh* (female sterile homeotic) of *Drosophila* and is phosphorylated as a consequence of this interaction (Platt *et al.*, 1999).

In the present study we aimed to characterize the high-resolution intranuclear distribution of RING3 in relation to LANA during different phases of the cell cycle and the effect of LANA on RING3 expression.

Methods

■ **Cell culture and transient transfection.** The cells were grown at 37 °C with 5% CO_2 in Iscove's modified Dulbecco's cell culture medium containing 10% foetal bovine serum, 2 mM L-glutamine, 100 U/ml penicillin and 100 U/ml streptomycin. The absence of mycoplasma contamination was examined routinely by Hoechst 33258 staining. The cell lines used in this study were the following: HHV-8-carrying human BC lines BC1, BCBL1; MCF7 human breast carcinoma; HeLa human cervical carcinoma; SW480 human colon carcinoma; ECV human endothelial cells; EBV-immortalized lymphoblastoid lines LCL 94C1 and LCL Nadia; Jurkat human T cell lymphoma; NKL92 human NK cell lymphoma; Burkitt lymphoma lines with different states of EBV latency, such as DG75 (EBV$^-$), Rael (EBV$^+$, type I), Raji (EBV$^+$, type III), Mutu I (EBV$^+$, type I), Mutu III (EBV$^+$, type III), Akata(−) (EBV$^-$) and Akata(+) (EBV$^+$, type I), as well as L mouse fibrosarcoma cells. Transient transfections of full-length LANA cDNA, inserted into a pcDNA1 vector were done according to the manufacturer's instructions using lipofectamin Plus reagent (GIBCO). Empty vector or a pBabe-EBNA-5 construct was used for control transfections. Construct containing GFP–LANA C terminus was described by Szekely *et al.* (1999).

■ **Immunofluorescence microscopy.** Cells grown on coverslips or centrifuged (cytospin) onto glass slides were fixed in methanol:acetone (1:1) at −20 °C for 20 min and then re-hydrated in PBS for 20 min at room temperature. The primary antibodies used in this study were human anti-LANA (antiserum collected from patients suffering from the classical form of Kaposi's sarcoma at the Dermatology Unit of Debrecen Medical School, Hungary; a gift from Attila Juhasz) and rabbit polyclonal anti-RING3 antibody (Platt *et al.*, 1999). Rhodamine-conjugated rabbit anti-human (DAKO) or FITC-conjugated swine anti-rabbit (DAKO) antibodies were used as secondary antibodies. Control transfection of pBabe-EBNA-5 was stained with a mouse monoclonal, JF186 (Finke *et al.*, 1987). Rhodamine-conjugated horse anti-mouse (Vector) was used as secondary antibody. The sera were diluted in blocking buffer (2% BSA, 0·2% Tween-20, 10% glycerol, 0·05% NaN_3 in PBS). Following a 1 h incubation at room temperature with primary antibody, the cells were washed three times in PBS and then incubated for 30 min with the secondary antibody. Double staining between LANA and RING3 was performed in the following order: rabbit anti-RING3, FITC-conjugated

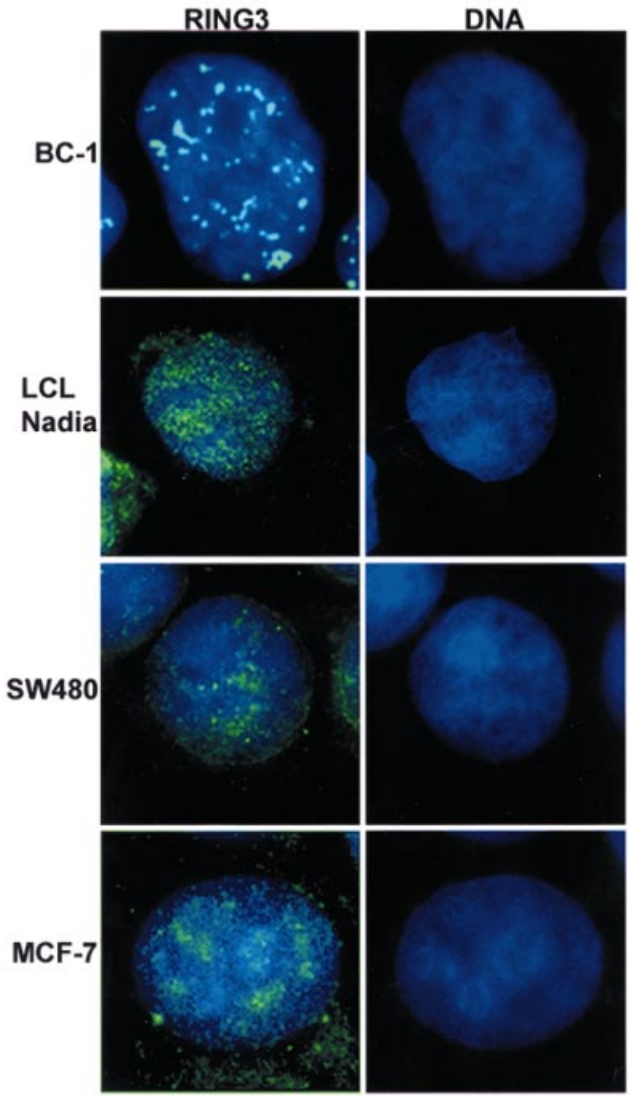

Fig. 1. Distribution of RING3 protein in different cell lines visualized by immunofluorescence staining with rabbit anti-RING3 antibody. Left column RING3 and DNA, right column DNA staining. Body cavity lymphoma line BC1 shows very intense nuclear staining associated with distinct nuclear bodies. Other cells lines show weak homogeneous or very fine speckled staining localized mainly to the euchromatin.

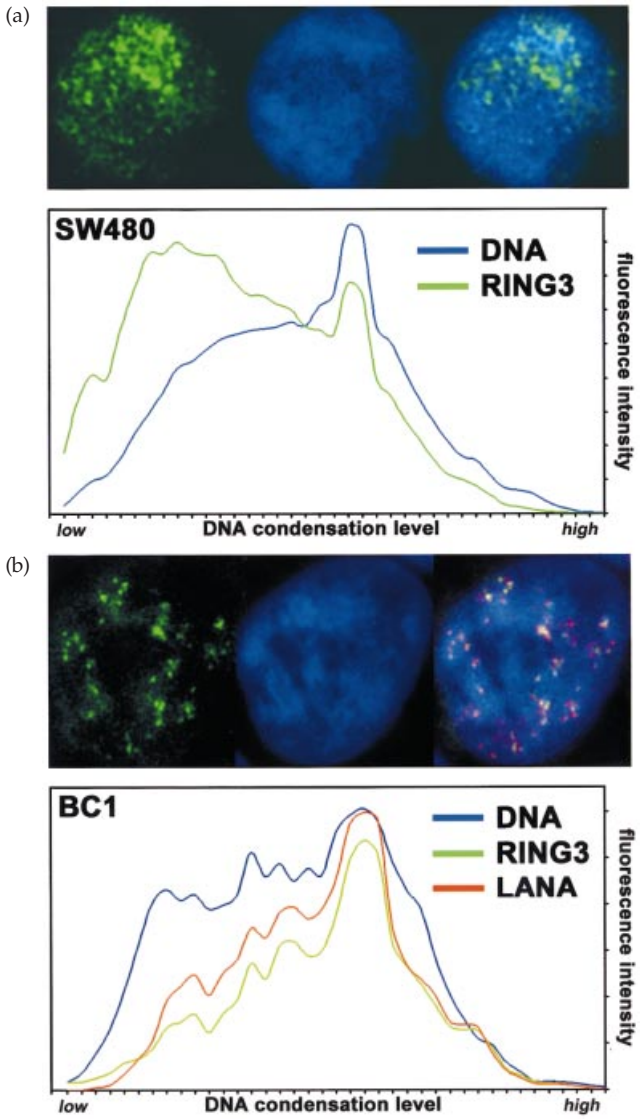

Fig. 2. RING3 (green) localizes to the euchromatin of the nucleus in virus-free SW480 but together with LANA (red) associates with the heterochromatin in latently infected KSHV/HHV-8 positive BC1 cells. The fluorescence intensity distribution as a function of DNA staining intensity level was calculated and plotted using the computer program CHROMATIN.

swine anti-rabbit serum, normal rabbit serum, human anti-LANA and rhodamine-conjugated rabbit anti-human serum. DNA was stained by Hoechst 33258 or by propidium iodide. Each incubation was followed by three washes in PBS. The coverslips or glass slides were mounted with 70% glycerol containing 2·5% DABCO anti-fading agent (Sigma). Images were collected using a Leitz DM RB microscope, equipped with Leica PL Fluotar 100 × and 40 × oil immersion objectives. Composite filter cubes were used for the FITC, Texas red/rhodamine and Hoechst 33258 fluorescence, respectively. The pictures were captured with a Hamamatsu dual mode cooled CCD camera (C4880), recorded and analysed on a Pentium PC computer equipped with an AFG VISION*plus*–AT frame grabber board using Hipic5.1.0 (Hamamatsu), Image-Pro Plus (Media Cybernetics). Digital images were assembled using Adobe Photoshop software. Optical sectioning and three-dimensional reconstitution was carried out using a Zeiss Axiophot microscope, equipped with 16 × oil Plan-Neofluar NA 0·5, 63 × oil Plan-Apochromat NA 1·4 and 100 × oil Plan-Neofluar NA 0·7–1·3 objectives, illuminated with an Osram HBO 100 W mercury short arc lamp. The following excitation filters, mounted in the computer-controlled filter wheel, were used in this study: single band UV exciter for Hoechst (84360), single band blue exciter for FITC (84490), single band green exciter for TRITC (84555). The emission filter was a multiple band pass filter (84000) mounted on a static stage. All filters were purchased from Chroma Technology. The filter wheel, dual shutter and Z axis motor were controlled through a LEP MAC2000 Communication Interface 73000400 using an RS-232 serial connection (all devices from Ludl Electric Products). Images were captured with a PXL cooled CCD camera (Photometrix) operating at −25 °C, using 12 bit (4096 greyscale level) capture mode. The hardware control and image processing was provided by a Pentium PC computer equipped with a 600 MHz Pentium III processor and

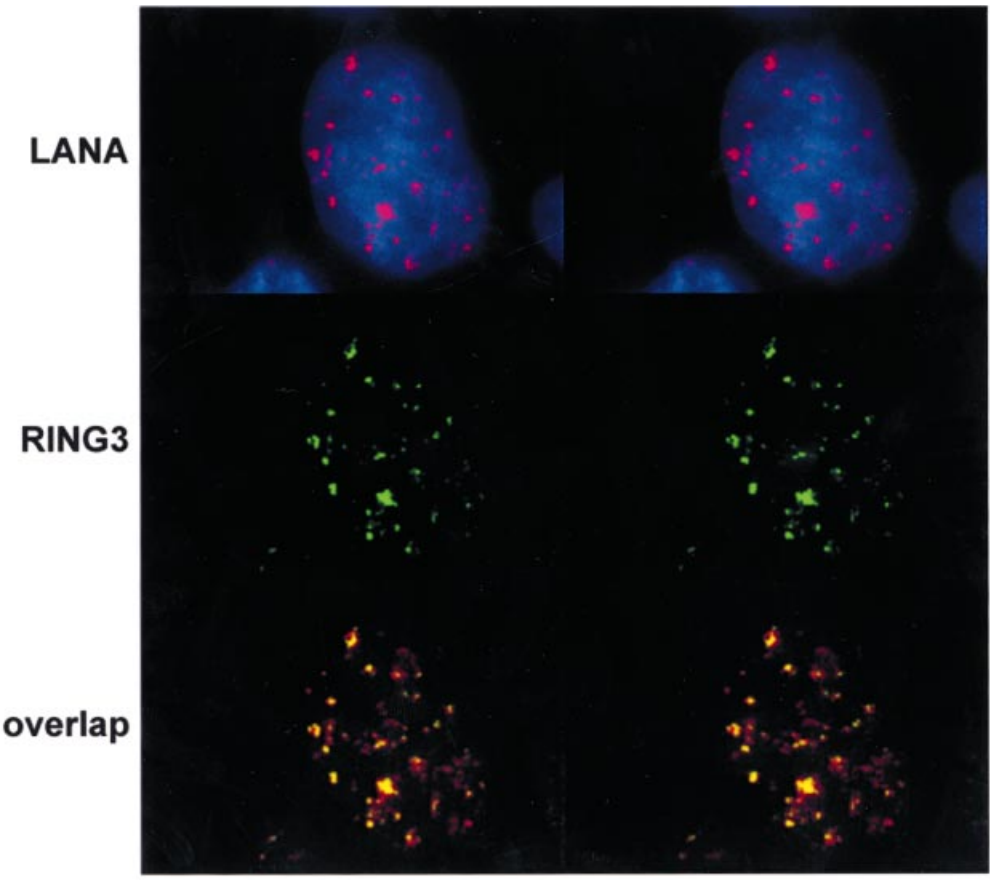

Fig. 3. The bulk of LANA co-localizes with the bulk of RING3 in the nuclear bodies of BCBL1 cells as shown on the three-dimensional reconstitution of an optically sectioned nucleus (11 sections 0·2 μm apart). LANA (red), RING3 (green), DNA (blue), co-localization (yellow). To preserve the depth perspective, the maximum intensity projection algorithm was used on the individually de-blurred optical sections, creating stereo pictures. The effect of a stereo-image is achieved by crossed eyes, producing a third image between the left and right panels, or with the help of stereoscopic glasses.

512 Mb RAM. The operation system was LINUX Mandrake 7.0. The imaging programs were written and operated using the ISee 5.1 graphical programming system (Inovision). Our program ST-FITC-Rhodamine-Hoechst-bin1 was a novel hybrid version of TROOPER3 and STEREOTROOPER (Holmvall & Szekely, 1999) that produces both single and stereo-projected three-colour images from a series of wide-field pictures where the out-of-focus blur was removed by nearest neighbour de-convolution and the resulting images were built up using a maximum intensity projection algorithm. This novel program also automatically compensated for any shining through from FITC, TRITC and Hoechst 33258 colour channels. The program CHROMATIN (Holmvall & Szekely, 1999) was used on individual optical sections created by the program ST-FITC-Rhodamine-Hoechst t-bin1.

■ **Ratio RT–PCR assay.** mRNA was isolated from pCDNA4-LANA-transfected and pCDNA4 MCF7 cell lines after 0 h, 24 h, 36 h and 72 h using Dynabeads (Dynal) according to the manufacturer's recommendation. The mRNA samples were eluted in 20 μl water. Ten μl of the mRNA samples was reverse-transcribed with Superscript II (Life Technologies) according to the manufacturer's recommendation in a 20 μl volume using oligo$(dT)_{30}$ primer. The RT–PCR reactions were performed on a Rapidcycler (Idahotech) capillary PCR machine in a 10 μl volume. The amplification reactions contained 0·5 μl of cDNA template, 50 mM Tris pH 8·0, 500 μg/ml BSA, 3 mM $MgCl_2$, 200 μM dNTP, 0·3 μM of GAPDH primers (GPDH5↔5′ ACCACAGTCCATGCCATCAC 3′; GPDH3↔5′ TCCACCACCCTGTTGCTGTA 3′), 1 μM of RING3 primers (RING35↔5′ AGTCCTTGCACTCTGCTGGA 3′; RING33↔5′ GTGCTGCCTTAGGCTCAAGA 3′) and 0·4 U Platinum Taq polymerase (Life Technologies). The reactions were cycled 27, 30 and 33 times, after an initial 15 s denaturation at 94 °C, under the following conditions: 94 °C, 0 s; 55 °C, 0 s; 72 °C, 30 s. The PCR products were separated on a 2·5% agarose gel in 1 × TAE buffer in the presence of 10 μg/ml ethidium bromide. The bands were visualized in an Intelligent Dark Box II (FujiFilm) and quantified using ImageGauge 3.122 software (FujiFilm).

Results

RING3 accumulates in nuclear bodies in HHV-8-positive BC cells but not in virus-negative cells

Immunofluorescence staining of different cells lines with rabbit antibodies raised against the RING3 protein showed either weak homogeneous or a fine speckled pattern in most of the lines studied (Table 1 and Fig. 1). In KSHV/HHV-8-negative cell lines RING3 predominantly localized to nuclear areas with low DNA condensation levels (Figs 1 and 2a).

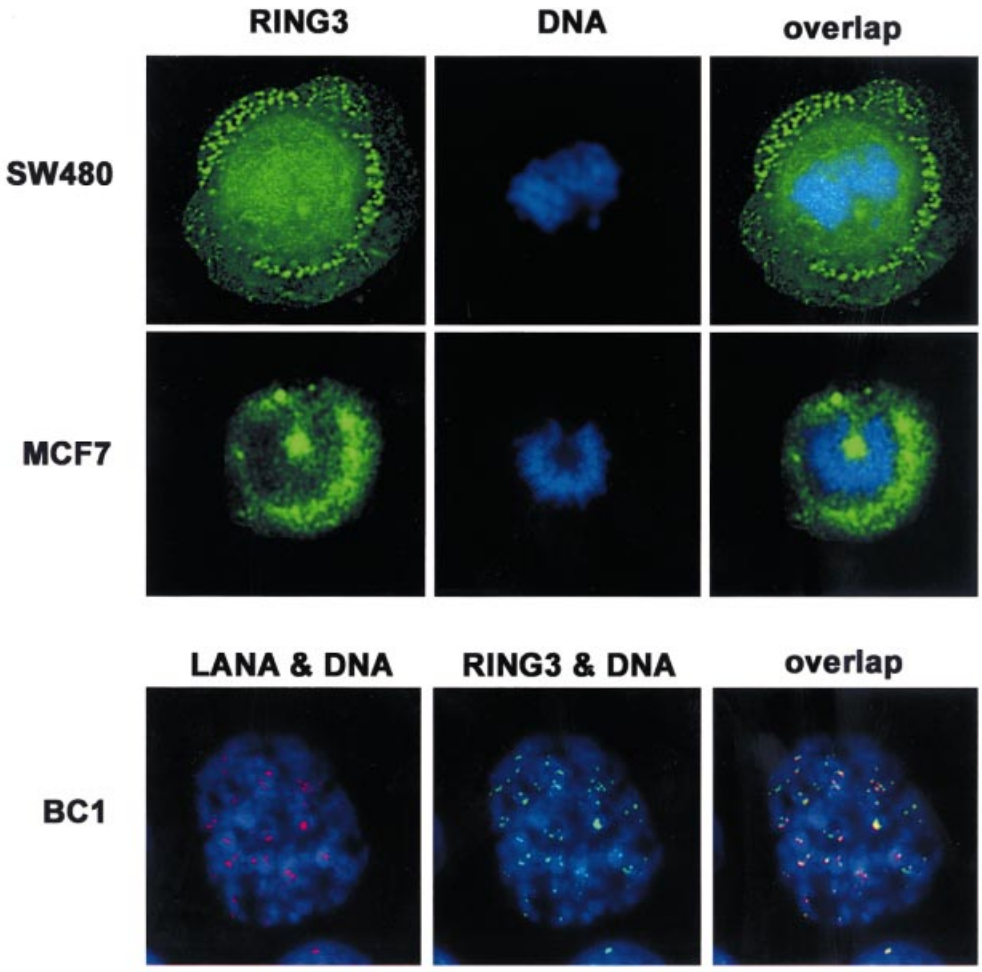

Fig. 4. RING3 dissociates from the chromosomes of the mitotic cell of uninfected SW480 and MCF7 cell lines but remains associated with the chromosomes of the KSHV/HHV-8-positive BCBL1 cells, where it co-localizes with LANA.

In contrast HHV-8-positive BC lines BC1 and BCBL1 showed intense RING3 staining localizing to LANA like nuclear bodies that associated with the heterochromatin. This differential localization was further confirmed by analysing HHV-8-negative (SW480) and -positive (BC1) nuclei with the help of our computer program CHROMATIN. We used out-of-focus blur-free optical sections of nuclei as input for the analysis. The program created a 40 step scale of the blue fluorescence intensities of bisbenzidine-stained nuclei and calculated the total amount of green (RING3), red (LANA) and blue (DNA) signals corresponding to the pixels that belonged to the individual levels of the scale. In the SW480 cells the majority of the RING3 staining was associated with areas with low DNA condensation levels (on the left side of the DNA distribution curve) (Fig. 2a), whereas in BC1 nuclei the majority of the RING3 signal was primarily associated with the high DNA density areas (had the maximal peak at the right side of the DNA distribution curve). In BC1 cells RING3 showed an almost identical distribution to LANA (Fig. 2b). Double immunofluorescence staining of LANA and RING3 showed an almost complete co-localization between the two proteins. The co-localization was further confirmed by optical sectioning and three-dimensional reconstitution of double-stained cell nuclei (Fig. 3).

Controls included in the double fluorescence staining experiments involved replacing the LANA-specific primary antibody with normal human serum or human serum reacting with nucleolar antigens and alternatively replacing the antibody to RING3 with normal rabbit serum.

As previously reported (Szekely *et al.*, 1999; Ballestas *et al.*, 1999), LANA remains associated with the chromosomes during mitosis. In view of the co-localization of LANA with RING3 in interphase cells we investigated the distribution of RING3 in KSHV/HHV-8-infected and -uninfected metaphase cells. As shown in Fig. 4, RING3 relocates from the euchromatin-containing regions of the interphase nucleus of KSHV/HHV-8-uninfected cells to the cytoplasm during mitosis. In marked contrast, in KSHV/HHV-8-infected cells RING3 remains associated with mitotic chromosomes where it co-localizes almost perfectly with LANA. These findings

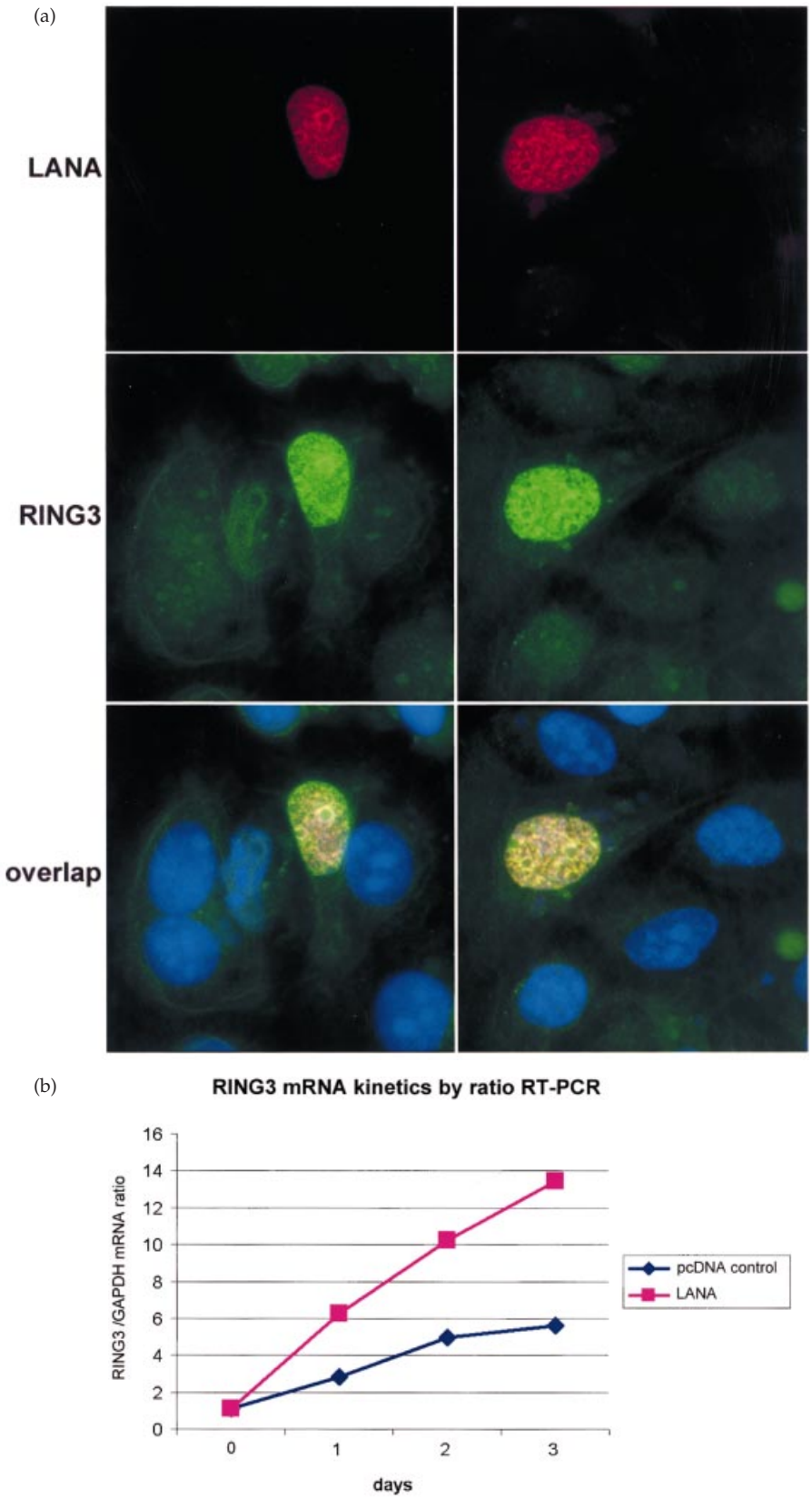

Fig. 5. (a) Transfection of LANA induces the increased expression of RING3 in an MCF7 human cell line as shown by double immunofluorescence staining. LANA (red), RING3 (green), DNA (blue). (b) Transfection of LANA induces increased expression of RING3 mRNA as shown by RING3/GAPDH ratio RT–PCR as a function of time (*x* axis) and RING3/GAPDH ratio (*y* axis).

indicate that the previously demonstrated (Platt *et al.*, 1999) interaction of LANA with the ET domain of RING3 is strong enough to relocate RING3 almost completely to mitotic chromosomes during anaphase.

LANA induces increased expression of RING3

In addition to its relocation to LANA-containing nuclear bodies RING3 appeared to stain much more strongly in KSHV/HHV-8-infected than in -uninfected cells. This could suggest either a stabilization and accumulation of RING3 in these structures, or that the presence of the virus or even LANA itself might induce RING3 expression. As shown in Fig. 5(a), transfection into MCF7 cells of a plasmid directing the expression of full-length LANA from a CMV promoter resulted in increased immunofluorescence staining for RING3. The same result was obtained when LANA was introduced into SW480 human colon carcinoma or L mouse fibrosarcoma cells. No increased RING3 expression was observed when the C-terminal 182 amino acids were expressed as a part of a GFP fusion protein (data not shown).

LANA has recently been shown to induce several cellular genes (Renne *et al.*, 2001) and RING3 was shown to be up-regulated in response to parasitic infections (Lau *et al.*, 2001). To examine the possibility that LANA might induce expression of the RING3 gene, we carried out ratio PCR by quantifying RING3 and glyceraldehyde-3-phosphate dehydrogenase (GAPDH) RT–PCR products from the same reaction mixture after different numbers (30, 33, 36) of amplification cycles. These experiments were carried out at different time-points (24, 48, 72 h) after transfection and were compared with RING3/GAPDH ratios from empty vector-transfected cells. These experiments clearly showed an increase of RING3 mRNA levels in LANA-transfected cultures (Fig. 5b).

LANA and RING3 form nuclear bodies in transfected cells even in the absence of the viral genome and lead to the dissolution of heterochromatin

LANA anchors HHV-8 DNA to the host chromatin. Introduction of a plasmid with the KSHV/HHV-8 latent origin of replication into LANA-expressing BJAB cells leads to the formation of distinct nuclear bodies (Ballestas *et al.*, 1999). After transfecting LANA into MCF7 and SW480 cells we observed that a fraction of cells produced a stippled nuclear staining pattern. Double immunofluorescence staining and three-dimensional reconstitution from a series of optical sections showed that in these KSHV/HHV-8-negative cells transfected LANA also co-localized with RING3 in focal aggregates reminiscent of the nuclear bodies that are present in latent virus-harbouring cells (Fig. 6a). These focal aggregates regularly associated with the perinucleolar heterochromatin in human cells. High magnification images of the perinucleolar regions of the transfected cells showed decreased local DNA staining at the sites of focal LANA aggregates (Fig. 6b). Interestingly, in cells that showed high levels of LANA expression with homogeneous nuclear distribution, the peri-

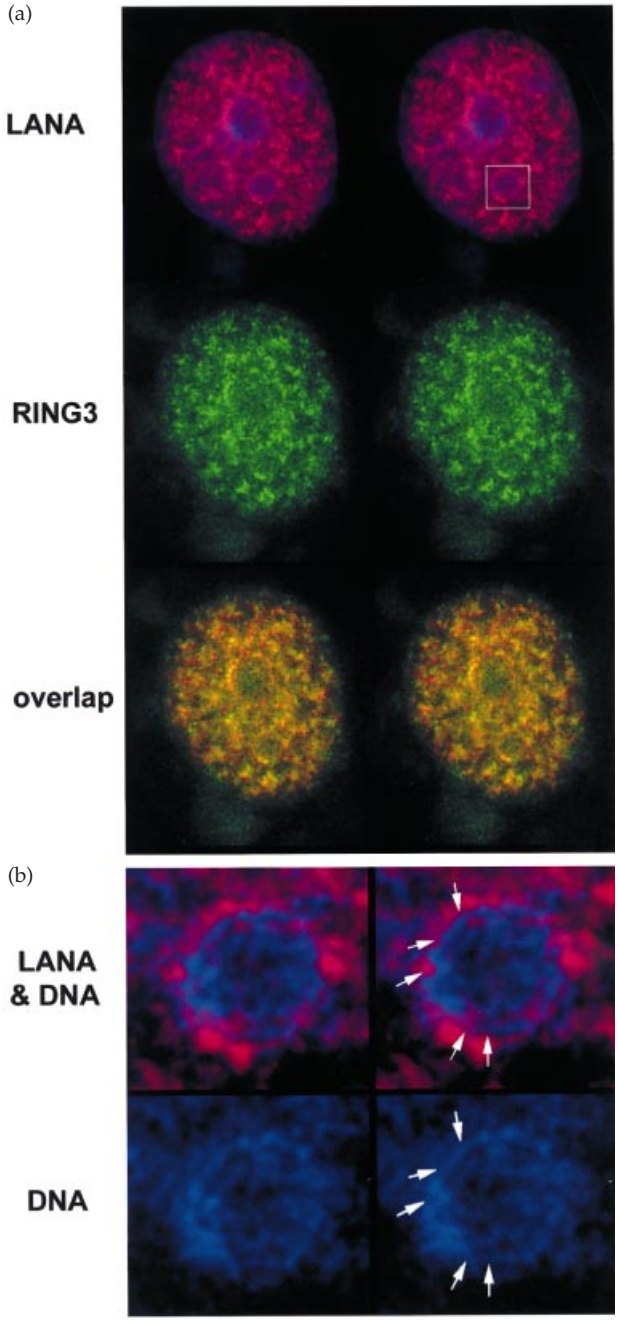

Fig. 6. (a) Co-localization of LANA and LANA-induced RING3 in transfected MCF7 cells as shown by stereo-projection of three-dimensional reconstituted double-stained nuclei (11 sections 0·2 μm apart). LANA (red), RING3 (green), DNA (blue), co-localization (yellow). (b) LANA-positive foci concentrate at areas of eroded perinuclear heterochromatin (white arrows). Stereo-projected three-dimensional magnified image corresponding to the area demarked by the white box in (a).

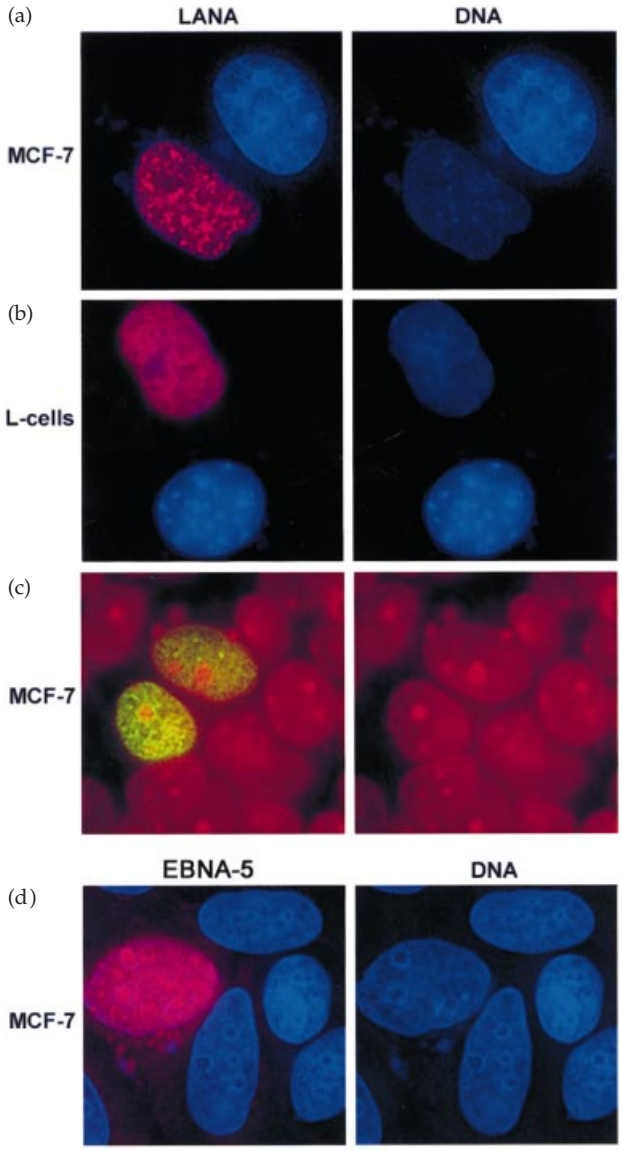

Fig. 7. Transfection of LANA leads to the dissolution of perinucleolar heterochromatin in human MCF7 (a) and pericentromeric heterochromatin in mouse L cells (b). LANA (red), DNA (blue). MCF7 cells transfected with high levels of LANA (c, green) and stained with propidium iodide (red) did not show any alteration in DNA staining intensity. MCF7 cells transfected with high levels of EBV-encoded EBNA-5 (d, red) and stained with Hoechst 33258 (blue) were used as a control transfection.

nucleolar heterochromatin completely disappeared. Because it is difficult to clearly demarcate the euchromatin/heterochromatin borders in human cells we examined mouse L cells, in which the heterochromatin forms very distinct blob-like structures. Transfection of LANA produced mainly intense homogeneous nuclear staining in the L cells with the almost complete disappearance of heterochromatin (Fig. 7). Interestingly both mouse and human cells that expressed high levels of exogenous LANA and induced RING3 showed decreased overall staining with the DNA-binding dye bisbenzidine (Hoechst 33258), which binds to the AT-rich minor groove (Fig. 7a, b) but not with the interchelating dye propidium iodide (Fig. 7c, propidium iodide staining in red), indicating that the decrease in staining intensity was not due to DNA degradation. As a control we overexpressed EBNA-5 in MCF7 cells (Pokrovskaja *et al.*, 2001). EBNA-5 did not induce any visible change in the chromatin distribution or bisbenzidine staining intensity (Fig. 7d). Control experiments were performed in which Hoechst 33258 was added in various incubation steps to exclude the possibility that the staining order affected the binding of Hoechst to DNA. Independently of staining order, the overall DNA staining was decreased in the LANA-expressing cells.

Discussion

Yeast two-hybrid screening identified RING3, a human homologue of the *Drosophila fsh* gene, as a binding partner of LANA. The binding was further confirmed by GST pull-down and co-immunoprecipitation assays. Association of RING3 with LANA leads to the phosphorylation of LANA through the recruitment of an as yet unidentified kinase (Platt *et al.*, 1999).

RING3 is a member of the family of bromodomain-containing proteins that include the SWI/SNF-type chromatin remodelling proteins, histone acetylases and CBP/p300 CREB-binding co-activators. NMR studies on the structure of bromodomain suggested that four of them form alpha-helix bundles that may serve as a chromatin-targeting module that can interact specifically with acetylated lysines (Dhalluin *et al.*, 1999).

RING3 belongs to the BET subgroup of bromodomain proteins, members of which contain two bromodomains and an ET motif, a protein–protein interactive surface. This group also includes, besides the *Drosophila* fsh, the yeast BDF proteins that regulate transcription through interaction with general transcription factors.

The human genome encodes at least four additional BET subgroup proteins: BRDT, ORFX, MCAP and HUNK1 (Jones *et al.*, 1997; Dey *et al.*, 2000). Interestingly the gene encoding RING3 is the only gene of the MHC class II region of human 6p21.3 that is not obviously associated with the immune system (Beck *et al.*, 1996).

The function of RING3 is as yet poorly understood. In *Drosophila*, fsh is implicated in the establishment of the segments in the early embryo (Beck *et al.*, 1992) by interacting with the trithorax pathway (Mozer & Dawid, 1989).

The murine RING3 homologue (Fsrg1) may play a regulatory role in folliculogenesis and in the hormone-dependent remodelling of epithelia (Rhee *et al.*, 1998). RING3 is expressed at high levels in testis and may also play a role in the regulation of spermatogenesis (Taniguchi *et al.*, 1998). A recent report found that RING3 expression was increased in several organs as a result of parasite infection, suggesting that

it could represent an early response gene involved in the innate immune response (Lau *et al*., 2001). In the present paper we also show that LANA activates RING3 gene expression.

We also show that in KSHV/HHV-8-uninfected cells RING3 localizes to euchromatin regions in the interphase nucleus. During mitosis, RING3 appears to be released to the cytoplasm, similar to other transcription regulators, e.g. CBP, SP1, TFIIB (Dey *et al*., 2000). In this respect RING3 differs from another recently described human member of the *fsh* family, MCAP, which has recently been reported to be located in heterochromatin regions and to remain associated with condensed chromosomes during mitosis (Dey *et al*., 2000). This difference in the sub-cellular localization of RING3 and MCAP may point to different functional roles. Interestingly, MCAP contains a long C-terminal extension, absent in RING3, distal from the ET domain, which characterizes all members of the *fsh* family.

We found that the bulk of RING3 co-localizes with the bulk of LANA in the nuclear bodies of KSHV/HHV-8-positive BC cells. These LANA-positive nuclear bodies are located on the euchromatin/heterochromatin interface in BC cells or in human–mouse hybrids. This localization is preserved when LANA is produced from an exogenously introduced expression vector. This markedly different localization of RING3 in KSHV/HHV-8-infected versus -uninfected cells strongly suggests that its interaction with LANA, previously demonstrated biochemically (Platt *et al*., 1999), is strong enough to quantitatively relocate RING3 to sub-nuclear structures containing KSHV/HHV-8 episomal DNA and LANA.

Importantly, however, high level expression leads to the dissolution of both human and mouse heterochromatin with accompanying bisbenzidine (Hoechst 33258) but not propidium iodide hypochromazia. Bisbenzidine binds to the minor grooves of AT-rich DNA. Culturing mouse cells in the presence of bisbenzidine inhibits the chromatin condensation of the pericentromeric heterochromatin. The staining difference between bisbenzidine and the interchelating dye propidium iodide indicates that DNA is preserved in the transfected cells and bisbenzidine hypochromazia is not a result of selective DNA degradation. Another possible explanation for this phenomenon is that association of LANA or RING3–LANA complexes with DNA leads to decreased accessibility of minor grooves. However, the images presented in Figs 5(a), 6, 7 are more likely to indicate that LANA–RING3-containing heterochromatin regions show signs of heterochromatin dissolution.

We suggest that in virus-infected cells the LANA–RING3 nuclear bodies create a local microenvironment where the viral DNA is anchored to host heterochromatin but heterochromatization is inhibited in the immediate neighbourhood of the viral DNA LANA and/or RING3.

We thank Dr M. Oren, The Weizmann Institute of Science, Israel for the MCF7 cells. This work was supported by The Swedish Cancer Society, Sweden and Cancer Research Institute/Concern Foundation.

References

Ballestas, M. E., Chatis, P. A. & Kaye, K. M. (1999). Efficient persistence of extrachromosomal KSHV DNA mediated by latency-associated nuclear antigen. *Science* **284**, 641–644.

Beck, S., Hanson, I., Kelly, A., Pappin, D. J. & Trowsdale, J. (1992). A homologue of the Drosophila female sterile homeotic (fsh) gene in the class II region of the human MHC. *DNA Sequence* **2**, 203–210.

Beck, S., Belich, M., Gruneberg, U., Jackson, A., Kelly, A., Sanseau, P., Sanderson, F., Trowsdale, J. & Van Ham, M. (1996). Organisation and functions of class II genes and molecules. *DNA Sequence* **7**, 21–23.

Boshoff, C. & Weiss, R. A. (1998). Kaposi's sarcoma-associated herpesvirus. *Advances in Cancer Research* **75**, 57–86.

Cotter, M. A., II & Robertson, E. S. (1999). The latency-associated nuclear antigen tethers the Kaposi's sarcoma-associated herpesvirus genome to host chromosomes in body cavity-based lymphoma cells. *Virology* **264**, 254–264.

Dey, A., Ellenberg, J., Farina, A., Coleman, A. E., Maruyama, T., Sciortino, S., Lippincott-Schwartz, J. & Ozato, K. (2000). A bromodomain protein, MCAP, associates with mitotic chromosomes and affects G2-to-M transition. *Molecular and Cellular Biology* **20**, 6537–6549.

Dhalluin, C., Carlson, J. E., Zeng, L., He, C., Aggarwal, A. K. & Zhou, M. M. (1999). Structure and ligand of a histone acetyltransferase bromodomain. *Nature* **399**, 491–496.

Dupin, N., Fisher, C., Kellam, P., Ariad, S., Tulliez, M., Franck, N., van Marck, E., Salmon, D., Gorin, I., Escande, J. P., Weiss, R. A., Alitalo, K. & Boshoff, C. (1999). Distribution of human herpesvirus-8 latently infected cells in Kaposi's sarcoma, multicentric Castleman's disease, and primary effusion lymphoma. *Proceedings of the National Academy of Sciences, USA* **96**, 4546–4551.

Finke, J., Rowe, M., Kallin, B., Ernberg, I., Rosen, A., Dillner, J. & Klein, G. (1987). Monoclonal and polyclonal antibodies against Epstein–Barr virus nuclear antigen 5 (EBNA-5) detect multiple protein species in Burkitt's lymphoma and lymphoblastoid cell lines. *Journal of Virology* **61**, 3870–3878.

Friborg, J., Jr, Kong, W., Hottiger, M. O. & Nabel, G. J. (1999). p53 inhibition by the LANA protein of KSHV protects against cell death. *Nature* **402**, 889–894.

Holmvall, P. & Szekely, L. (1999). Computer programs that allow fast acquisition, visualization and overlap quantitation of fluorescent 3D microscopic objects using nearest neighbor deconvolution algorithm. *Applied Immunohistochemistry & Molecular Morphology* **7**, 226–236.

Jones, M. H., Numata, M. & Shimane, M. (1997). Identification and characterization of BRDT: a testis-specific gene related to the bromodomain genes RING3 and Drosophila fsh. *Genomics* **45**, 529–534.

Katano, H., Sato, Y., Kurata, T., Mori, S. & Sata, T. (1999). High expression of HHV-8-encoded ORF73 protein in spindle-shaped cells of Kaposi's sarcoma. *American Journal of Pathology* **155**, 47–52.

Kedes, D. H., Lagunoff, M., Renne, R. & Ganem, D. (1997). Identification of the gene encoding the major latency-associated nuclear antigen of the Kaposi's sarcoma-associated herpesvirus. *Journal of Clinical Investigation* **100**, 2606–2610.

Kellam, P., Boshoff, C., Whitby, D., Matthews, S., Weiss, R. A. & Talbot, S. J. (1997). Identification of a major latent nuclear antigen, LNA-1, in the human herpesvirus 8 genome. *Journal of Human Virology* **1**, 19–29.

Krithivas, A., Young, D. B., Liao, G., Greene, D. & Hayward, S. D. (2000). Human herpesvirus 8 LANA interacts with proteins of the mSin3 corepressor complex and negatively regulates Epstein–Barr virus gene expression in dually infected PEL cells. *Journal of Virology* **74**, 9637–9645.

Lau, A. O. T., Sacci, J. B. & Azad, A. F. (2001). Host responses to *Plasmodium yoelii* hepatic stages: a paradigm in host–parasite interaction. *Journal of Immunology* **166**, 1945–1950.

Mozer, B. A. & Dawid, I. B. (1989). Cloning and molecular characterization of the trithorax locus of Drosophila melanogaster. *Proceedings of the National Academy of Sciences, USA* **86**, 3738–3742.

Platt, G. M., Simpson, G. R., Mittnacht, S. & Schulz, T. F. (1999). Latent nuclear antigen of Kaposi's sarcoma-associated herpesvirus interacts with RING3, a homolog of the Drosophila female sterile homeotic (fsh) gene. *Journal of Virology* **73**, 9789–9795.

Pokrovskaja, K., Mattsson, K., Kashuba, E., Klein, G. & Szekely, L. (2001). Proteasome inhibitor induces nucleolar translocation of the EBV-encoded EBNA-5. *Journal of General Virology* **82**, 345–358.

Radkov, S. A., Kellam, P. & Boshoff, C. (2000). The latent nuclear antigen of Kaposi sarcoma-associated herpesvirus targets the retinoblastoma–E2F pathway and with the oncogene Hras transforms primary rat cells. *Nature Medicine* **6**, 1121–1127.

Rainbow, L., Platt, G. M., Simpson, G. R., Sarid, R., Gao, S. J., Stoiber, H., Herrington, C. S., Moore, P. S. & Schulz, T. F. (1997). The 222- to 234-kilodalton latent nuclear protein (LNA) of Kaposi's sarcoma-associated herpesvirus (human herpesvirus 8) is encoded by orf73 and is a component of the latency-associated nuclear antigen. *Journal of Virology* **71**, 5915–5921.

Renne, R., Barry, C., Dittmer, D., Compitello, N., Brown, P. O. & Ganem, D. (2001). Modulation of the cellular and viral gene expression by the latency-associated nuclear antigen of Kaposi's sarcoma-associated herpesvirus. *Journal of Virology* **75**, 458–468.

Rhee, K., Brunori, M., Besset, V., Trousdale, R. & Wolgemuth, D. J. (1998). Expression and potential role of Fsrg1, a murine bromodomain-containing homologue of the Drosophila gene female sterile homeotic. *Journal of Cell Science* **111**, 3541–3550.

Szekely, L., Chen, F., Teramoto, N., Ehlin-Henriksson, B., Pokrovskaja, K., Szeles, A., Manneborg-Sandlund, A., Löwbeer, M., Lennette, E. T. & Klein, G. (1998). Restricted expression of Epstein–Barr virus (EBV)-encoded, growth transformation-associated antigens in an EBV- and human herpesvirus type 8-carrying body cavity lymphoma line. *Journal of General Virology* **79**, 1445–1452.

Szekely, L., Kiss, C., Mattsson, K., Kashuba, E., Pokrovskaja, K., Juhasz, A., Holmvall, P. & Klein, G. (1999). Human herpesvirus-8-encoded LNA-1 accumulates in heterochromatin-associated nuclear bodies. *Journal of General Virology* **80**, 2889–2900.

Taniguchi, Y., Matsuzaka, Y., Fujimoto, H., Miyado, K., Kohda, A., Okumura, K., Kimura, M. & Inoko, H. (1998). Nucleotide sequence of the ring3 gene in the class II region of the mouse MHC and its abundant expression in testicular germ cells. *Genomics* **51**, 114–123.

Received 9 July 2001; Accepted 12 September 2001